

Experimental investigation of optical discharge plasma in air in the presence of particles

V.I. Bukatyi and O.V. Gas'kova

Altai State University, Barnaul

Received February 28, 2001

We study the optical discharge in air in the presence of an absorbing carbon particle under the action of Nd laser radiation at the wavelength of $1.06\ \mu\text{m}$. Formation of secondary particles has been detected; these particles having the size from 0.01 to $1.2\ \mu\text{m}$ were generated in the processes of fragmentation, recondensation, and others. The particle size distribution histogram has been constructed based on microphotos. The dependence of the squared speed of the discharge front on the energy deposition has been found. The electron concentration has been determined using an electric sonde. The amplitude of pressure in the sonic wave is estimated.

Propagation of high-power laser radiation in air is accompanied, at certain radiation intensity, by the appearance of a breakdown zone. Immediately after the optical discharge was discovered, it was noticed that it has a threshold character. This means that as the radiation intensity decreases below a certain (threshold) value, no breakdown occurs. Since this effect aroused significant interest, many experimental data on the threshold intensity were obtained.¹⁻⁵ It was revealed that the threshold intensity depends on pressure, radiation wavelength, shape of a laser pulse, focusing geometry, ionization potential of gas atoms, and other parameters. In all studies on determination of the breakdown threshold, the presence of plasma in the focal area was recorded by appearance of a visible flash.

Studies of threshold conditions for optical breakdown at various seeds attract considerable attention^{6,7} This is caused by the fact that the mechanism of formation of the initial plasma cell determines further evolution of the process. There are many different theoretical models used for interpretation of experimental data on threshold conditions of different types of the breakdown. There exist particular models for each specific type of the breakdown. An example is the theory of aerosol breakdown that was developed based on two concepts. The first one, the explosion concept, is based on the assumption that an aerosol particle during its inertial confinement has enough time to absorb the amount of energy sufficient for complete evaporation.⁸ The second concept, conditionally called the thermal one, considers heating of a particle, its evaporation, and development of ionization in the generated vapor cloud.^{1,3,4} These concepts were significantly improved, and now rather detailed mathematical models of interaction of an aerosol particle with laser radiation have been developed for both the diffusion and hydrodynamic conditions of evaporation.

An original idea on the mechanism of aerosol breakdown due to "jumping" electrons is described in

Ref. 9. Any electron, whose kinetic energy on a particle boundary exceeds the work function of the particle material and the energy needed to overcome the Coulomb force, can leave the particle surface. After leaving the surface, the electrons having this energy come back, wherefrom the name "jumping electrons" follows. Every such electron takes the energy of the electromagnetic field and gives it to the particle. This energy is consumed for particle heating. If a jumping electron collides with molecules of the ambient gas, then its energy comes to ionization of the gas. Thus, two channels of transformation of the laser beam energy arise: the first channel corresponds to the mechanism of thermal explosion, and the second corresponds to the mechanism of avalanche ionization.

One can separate out several stages in particle heating by laser radiation. First, the total energy of laser radiation is removed due to thermal conductivity until the temperature reaches some value T^* called the temperature of developed evaporation. Since that time, the energy of laser radiation comes entirely to evaporation, and the corresponding mode is called the mode of developed evaporation.¹⁰ Another characteristic temperature is the boiling or sublimation point of the particle material at a given pressure of the ambient gas T_b . At $T < T_b$ the generated vapor diffuses into the ambient gas, and the vapor-gas mixture is formed. The corresponding mode of evaporation is called the diffuse mode. At $T > T_b$ the vapor pressure exceeds the ambient pressure, and this mode is called hydrodynamic. The temperature of particle heating depends on the absorbed laser energy.

In Ref. 6, the optical breakdown in aerosols of carbon, aluminum, germanium, sodium chloride, alumina, and glass particles was studied experimentally. With the aluminum oxide, used as an example, it was shown that for relatively large particles from 1 to $70\ \mu\text{m}$ in diameter the breakdown threshold is independent of the particle size. The situation with the dependence of the breakdown threshold on the particle material is

more complicated. The measured evaporation thresholds are $\sim 5 \text{ J/cm}^2$ for absorbing carbon and alumina particles of $50 \mu\text{m}$ in diameter, 20 and 40 J/cm^2 for reflecting aluminum and transparent germanium particles, respectively, and more than 50 J/cm^2 for the transparent sodium chloride particles. Nevertheless, the thresholds of plasma breakdown initiation by particles of these materials, except for alumina, almost coincide. The occurrence of the breakdown is determined by the shape of the radiation pulse.¹¹ To

compare theory with experiment, the time when the plasma appears should be fixed for a laser pulse of a given shape.

At the particle concentration higher than 10^3 cm^{-3} , as the breakdown plasma arises, the incident radiation is completely screened. As this takes place, a part of the laser pulse energy passing the breakdown zone before the appearance of plasma q_{thr} characterizes the beam energy density needed for the initiation of the breakdown by aerosol particles.⁶

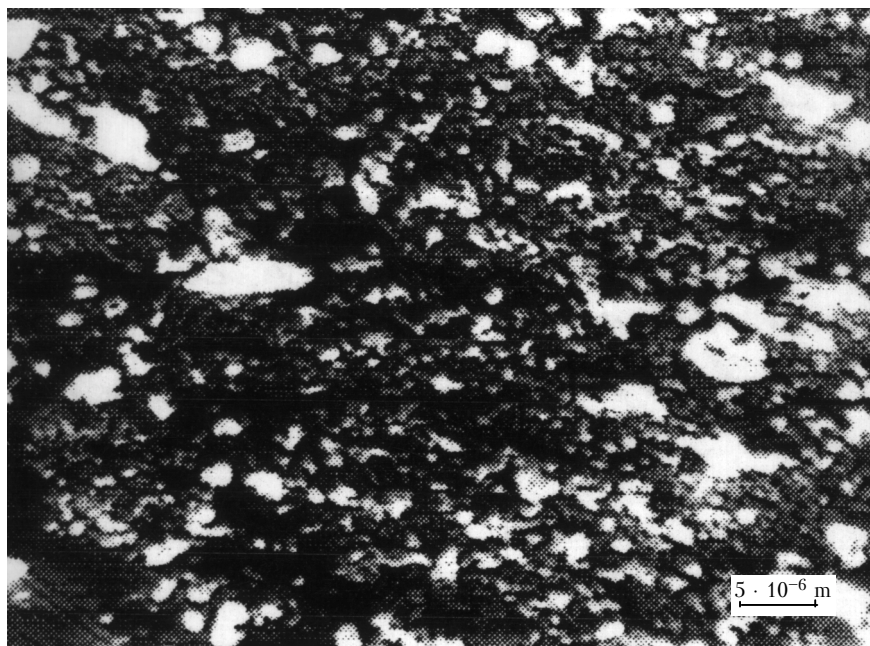


Fig. 1. Microphotos of carbon particles after exposure to laser radiation ($\times 4000$ magnification; pulse energy of 500 J).

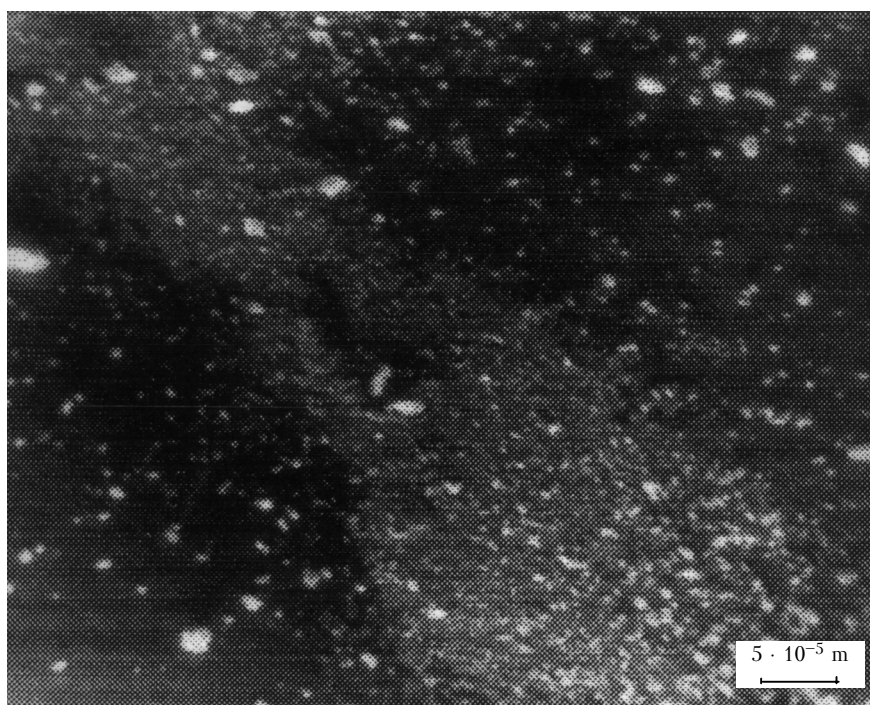


Fig. 2. Microphotos of carbon particles after exposure to laser radiation ($\times 4000$ magnification; pulse energy of 500 J).

The study of the plasma spectrum dynamics by a spectral method¹² shows that the state of plasma is close to the local thermodynamic equilibrium, because the available electron density is sufficient for maintaining the equilibrium between electrons and particles at the excited levels. Densitograms of radiation from the plasma formed at collective optical discharge in carbon aerosol showed that the emission spectra include lines of the excited nitrogen atoms NI and NII, oxygen atoms OI and OII, and carbon atoms CII. The electron concentration in the plasma calculated from the Stark broadening of NI and OI lines is $n_e \sim 10^{17} \text{ cm}^{-3}$. The plasma temperature determined from the ratio of the total intensities of lines belonging to the same element, but two neighboring degrees of ionization, proved to be 0.96–0.98 eV for nitrogen lines and 0.86 eV for the oxygen lines.

At the same time, the structure of secondary aerosol generated as a result of intense evaporation of the seed material and further recondensation at optical breakdown is still poorly understood.¹³ The aim of this study was the investigation of the structure of secondary particles generated in air in the presence of a carbon seed, as well as the main parameters of the formed plasma and accompanying effects.

As known, the aerosol of the nucleation mode ($d < 0.02 \mu\text{m}$) contributes significantly to microphysical parameters of the atmosphere. Therefore, we have undertaken an attempt to determine the size of particles generated at interaction of laser radiation with coarse aerosol particles. As to the mechanism of particle break in the field of high-power laser radiation, it was assumed^{14,17} that the inhomogeneity of the optical field inside the particle leads to its destruction and formation of smaller fragments, in which the field is homogeneous. The process of fragmentation of a reactor graphite particle was filmed in Ref. 15. Using the setup described in Ref. 16, we have conducted experiments to determine the size of secondary particles. A carbon particle about $500 \mu\text{m}$ in size was fixed on a quartz thread. When exposed to a pulse of the GOS-1001 Nd laser radiation with the wavelength of $1.06 \mu\text{m}$ and the pulse energy of 500 J, the processes of evaporation and recondensation resulting in the formation of smaller particles occurred; the newly formed particles were deposited onto a copper foil substrate. Photos of particles obtained with an electron microscope are shown in Figs. 1 and 2. The size distribution of the particles (from 0.01 to $1.2 \mu\text{m}$ with an insignificant part of larger particles) is shown in Fig. 3. In the experiments with the graphite particles about $200 \mu\text{m}$ in size, fragmentation was not observed. This can be explained by the fact that graphite particles evaporated completely during their inertial confinement in the focal area. Fragmentation of soot particles is explained in Ref. 15 by high porosity of these particles. Due to high porosity, the particle has no enough time to be warmed up thoroughly and breaks into small fragments.

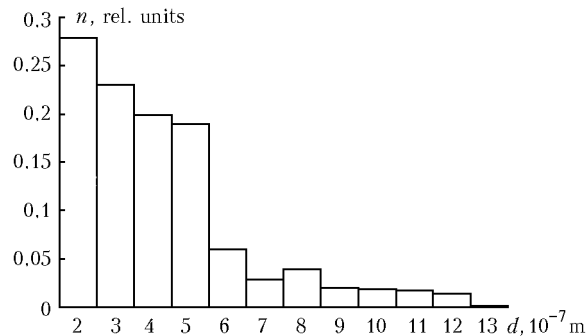


Fig. 3. Size-distribution histogram of secondary particles. Laser pulse energy of 500 J.

For an individual aerosol particle, the final stage of the optical discharge is expansion of the front separating the highly ionized gas from the undisturbed one.

The speed and mechanism of the front motion are determined by the intensity of a laser beam. Figure 4 shows the dependence of the discharge front speed on the laser pulse energy. The front speed was measured using the spectral method.

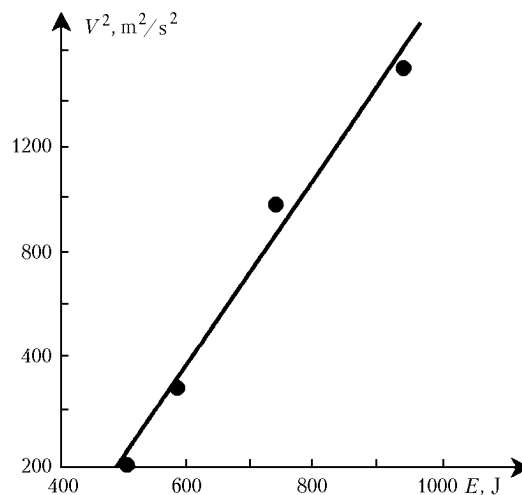


Fig. 4. Square speed of discharge front as a function of pulse energy.

The plasma front was recorded with a PMT recording glow in the oxygen line at 394 nm. This line was isolated with a MUM-2 monochromator. The spectrum was recorded through an aperture in the screen spaced by 6 mm from the focal area. The front speed was determined from the lag of a signal coming to a memory oscilloscope from the PMT relative to the laser trigger pulse. Because of the absence of devices measuring the power higher than 100 W, the radiation power in our case was measured by a standard power meter, which was set on backside of the acting laser. It recorded the radiation passed through the back mirror, whose reflection coefficient was 99.5%. This radiation consisted 0.5% of output laser radiation.

The measurements showed that the dependence of the squared speed on the pulse energy can be approximated by a linear function $V^2(E) = 3.69E - 746$. The equation for the discharge speed¹⁸ has the form

$$V^2 = V_0^2(R - 1),$$

where $R = E/E_{th}$, E is the laser pulse energy; E_{th} is the threshold energy; V_0 is a constant depending on the discharge parameters. Comparing these equations, we can find $V_0 = 41$ m/s, and the threshold energy is 475 J.

The electron concentration was measured by the sonde method. This method consists in measurement of the flux of charged particles onto a sonde placed in the plasma. Of interest for us is, first of all, conductivity of the plasma and the electron concentration connected with it, as well as fluctuations, time of appearance, existence, and decay of the plasma. This information can be obtained by use of the double-sonde method. To minimize the measurement error, the distance between the electrodes in the plasma should be no less than the distorted zone size. In the case of a double sonde, the distance between the electrodes should be larger than the maximum impact parameter

$$P_{max} \approx R_c(T_e/T_i),$$

where R_c is the radius of the volume charge layer; T_e is the electron temperature; T_i is the ion temperature. The Debye length can serve as a measure of extension of the volume charge. In Ref. 12 it is shown that the electron temperature differs insignificantly from the ion temperature, therefore the ratio T_e/T_i can be thought equal to unity. Thus, in our experiments we took the minimum distance between the electrodes equal to 0.005 m. The obtained oscillograms show that the plasma arises in 0.4 ms after the beginning of the pulse. The maximum conductivity of the plasma observed in the experiments was $\sigma = 0.2 \Omega^{-1} \cdot s^{-1}$. The measured conductivity corresponds to the electron concentration $n_e = 1.6 \cdot 10^{16} \text{ cm}^{-3}$.

Oscillations of the surface of the plasma channel induce a sonic wave. Analysis of oscillograms of microphone signals shows that a regular component with the characteristic frequency of 10^4 Hz is present in the spectrum of sonic oscillations. The level of sonic distortions was compared with the standard level of sonic oscillations of the same frequency generated by an audio-signal generator. The amplitude of pressure in the sonic wave measured in such a way was found to be ≈ 100 Pa 10 cm far from the discharge axis.

In conclusion, it can be noted that formation of secondary particles was found when studying the

optical discharge in air in the presence of an absorbing carbon particle. These particles were generated in the processes of fragmentation, recondensation, etc.; their size was from 0.01 to 1.2 μm . The dependence of the squared speed of the discharge front on the energy deposition has been found. The electron concentration has been determined ($n_e = 1.6 \cdot 10^{16} \text{ cm}^{-3}$) by the sonde method. The amplitude of pressure in the sonic wave has been estimated.

References

1. V.E. Zuev, Yu.D. Kopytin, and A.V. Kuzikovskii, *Nonlinear Optical Effects in Aerosols* (Nauka, Novosibirsk, 1980), 184 pp.
2. V.E. Zuev, A.A. Zemlyanov, Yu.D. Kopytin, and A.V. Kuzikovskii, *High-Power Laser Radiation in Atmospheric Aerosol* (Nauka, Novosibirsk, 1984), 184 pp.
3. Yu.M. Sorokin, I.Ya. Korolev, and E.M. Krikunova, *Kvant. Elektron.* **13**, No. 12, 2464–2473 (1986).
4. Yu.D. Kopytin, Yu.M. Sorokin, A.M. Skripkin, N.N. Belov, and V.I. Bukatyi, *Optical Discharge in Aerosols* (Nauka, Novosibirsk, 1990), 159 pp.
5. S.V. Zakharchenko and A.M. Skripkin, *Zh. Tekhn. Fiz.* **55**, No. 10, 1935–1942 (1985).
6. A.E. Negin, V.P. Osipov, and A.V. Pakhomov, *Kvant. Elektron.* **13**, No. 11, 2208–2215 (1986).
7. V.S. Vorob'ev and A.L. Khomkin, *Fiz. Plazmy* **10**, No. 5, 1025–1032 (1984).
8. F.V. Bunkin and V.V. Savranskii, *Zh. Eksp. Teor. Fiz.* **65**, No. 6(12), 2185–2195 (1973).
9. V.S. Vorob'ev, *Usp. Fiz. Nauk* **163**, No. 12, 51–83 (1993).
10. V.A. Vdovin and Yu.M. Sorokin, *Zh. Tekhn. Fiz.* **55**, No. 2, 319–325 (1985).
11. I.Yu. Borets-Pervak and V.S. Vorob'ev, *Kvant. Elektron.* **20**, No. 3, 264–270 (1993).
12. V.I. Bukatyi, K.I. Deines, and A.A. Tel'nikhin, *Atm. Opt.* **4**, No. 7, 538–540 (1991).
13. V.I. Bukatyi and K.V. Solomatin, *Izv. Altaiskogo Gosuniversiteta*, No. 7, 41–44 (1997).
14. N.N. Belov, *Kolloid. Zh.*, No. 5, 987–990 (1987).
15. V.V. Dar'yanov and V.N. Krasnopevtsev, in: *Interaction of High-Power Laser Radiation with Aerosol* (Novosibirsk, 1989) pp. 3–8.
16. V.I. Bukatyi and O.V. Gas'kova, *Atmos. Oceanic Opt.* **11**, No. 1, 39–41 (1998).
17. V.A. Pogodaev and A.E. Rozhdestvenskii, *Zh. Tekhn. Fiz.* **53**, No. 8, 1541–1546 (1983).
18. V.I. Bukatyi and A.A. Tel'nikhin, *Dynamics of Chaos and Order in Plasma-Radiation Systems* (Altai State University Publishing House, Barnaul, 1998), 123 pp.